HHS Public Access

Author manuscript

J Med Chem. Author manuscript; available in PMC 2021 June 07.

Published in final edited form as:

J Med Chem. 2012 January 12; 55(1): 515–527. doi:10.1021/jm2014277.

ADME-Guided Design and Synthesis of Aryloxanyl Pyrazolone Derivatives to Block Mutant Superoxide Dismutase 1 (SOD1) Cytotoxicity and Protein Aggregation: Potential Application for the Treatment of Amyotrophic Lateral Sclerosis

Tian Chen[1], **Radhia Benmohamed**[2], **Jinho Kim**[3], **Karen Smith**[4], **Daniel Amante**[3], **Richard I. Morimoto**[5], **Donald R. Kirsch**[2], **Robert J. Ferrante**[3], **Richard B. Silverman**[1,6,*]

[1]Department of Chemistry Northwestern University, Evanston, Illinois 60208-3113 USA

[2]Cambria Pharmaceuticals, Cambridge, Massachusetts, 02142 USA

[3]Neurological Surgery, Neurology, and Neurobiology Departments, University of Pittsburgh, Pittsburgh, PA 15213, USA and the Geriatric Research Educational and Clinical Center (00-GR-H), V.A. Pittsburgh Healthcare System, 7180 Highland Drive, Pittsburgh, PA 15206, USA

[4]Bedford VA Medical Center, 200 Springs Road, Bedford MA, 01730, USA

[5]Department of Molecular Biosciences, Rice Institute for Biomedical Research, Northwestern University, Evanston, Illinois 60208-3500 USA

[6]Department of Molecular Biosciences, Chemistry of Life Processes Institute, Center for Molecular Innovation and Drug Discovery, Northwestern University, Evanston, Illinois 60208-3113 USA

Abstract

Amyotrophic lateral sclerosis (ALS) is an orphan neurodegenerative disease currently without a cure. The arylsulfanyl pyrazolone (ASP) scaffold was one of the active scaffolds identified in a cell-based high throughput screening assay targeting mutant Cu/Zn superoxide dismutase 1 (SOD1)-induced toxicity and aggregation as a marker for ALS. The initial ASP hit compounds were potent and had favorable ADME properties, but had poor microsomal and plasma stability. Here, we identify the microsomal metabolite and describe synthesized analogs of these ASP compounds to address the rapid metabolism. Both *in vitro* potency and pharmacological properties of the ASP scaffold have been dramatically improved via chemical modification to the corresponding sulfone and ether derivatives. One of the ether analogs (**13**), with superior potency and *in vitro* pharmacokinetic properties, was tested *in vivo* for its pharmacokinetic profile, brain penetration, and efficacy in an ALS mouse model. The analog showed sustained blood and brain

*To whom correspondence should be addressed at the Department of Chemistry, Northwestern University, 2145 Sheridan Road, Evanston, IL 60208-3113. Phone: 1-847-491-5653. Fax: 1-847-491-7713. Agman@chem.northwestern.edu.

Supporting Information Available: Experimental details and data for **35**, **36**, **39**, **41** and **42–47**, HPLC data and spectra for **1**-**19**, HPLC spectra and data of microsomal stability of minaprine and **1**, data and spectra of metabolite profiling of **1** and **3**, bioanalysis data of *in vivo* mouse steady-state level study and *in vivo* blood brain barrier study of **13**, data for the effect of **13** on hERG potassium channel and data for the effect of **13** on enzymes and receptors. This material is available free of charge via the Internet at http://pubs.acs.org.

levels *in vivo* and improved activity in the mouse model of ALS, thus validating the new, aryloxanyl pyrazolone scaffold as an important novel therapeutic lead for the treatment of this neurodegenerative disorder.

Graphical Abstract

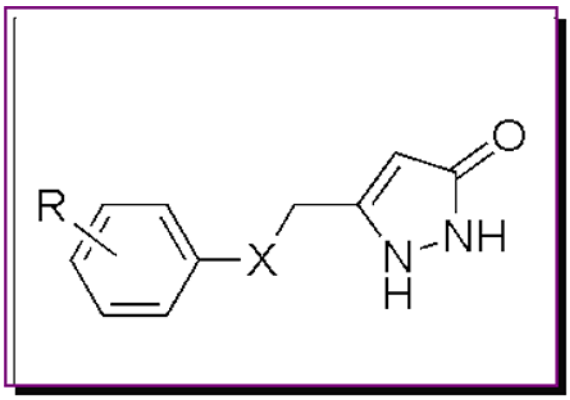

X = SO, SO_2, O
R = alkyl, aromatic and/or halogen groups

Introduction

Amyotrophic lateral sclerosis (ALS), also known as Lou Gehrig's disease, is a fatal neurodegenerative disease resulting in progressive muscle loss and paralysis.[1] The incidence of ALS is 1–2/100,000 per year,[2,3] with approximately 2–5 years from diagnosis to death. There is a disproportionate incidence of ALS among military personnel, particularly among Gulf War veterans.[4,5,6] No effective treatment for the disease is currently known.[7] Riluzole, the only FDA approved drug for treating ALS, extends patient lives by 2–3 months.[8]

The sporadic disease (SALS) accounts for approximately 90% of all cases and familial disease (FALS) the remaining 10%. Over 100 mutations in Cu/Zn superoxide dismutase 1 (SOD1) have been identified since the pioneering work of Brown and colleagues in identifying this FALS gene,[9] and studies on SOD1 have advanced the understanding of the molecular mechanisms and underlying pathogenesis of this disease.[10] Mutations in SOD1 are believed to be responsible for about 20% of all FALS cases.[11,12] The latter findings resulted in the development of transgenic mouse models, which have further elucidated pathophysiological mechanisms as well as provided a model for preclinical drug trials.[13] The clinical and pathological features of FALS and sporadic ALS are similar, which supports the strategy of using laboratory models of FALS mutations for elucidating disease pathogenesis and for identifying potential therapeutic targets for both forms of the disease.[14,15] Protein aggregation is a pathological hallmark of ALS[13,16] the appearance of intracellular inclusions containing detergent-insoluble SOD1 protein aggregates represents a common early event associated with SOD1 cellular toxicity.[17,1]

In previous studies, PC12 cells expressing mutant G93A SOD1 were utilized in a cell-based high throughput screening (HTS) assay.[18,19] The arylsulfanyl pyrazolone (ASP) scaffold was identified as one of the active scaffolds showing protection against cytotoxicity from protein aggregation from a 50,000-compound library screened in the HTS assay (Figure 1; two general structures were active, where Type II was, in general, more potent than Type I).[20] Structural optimization of this scaffold led via **1** (EC_{50} 1.93 μM) and **2** (EC_{50} 0.71 μM) to a more potent analog (**3**) than the original screening hits, with an EC_{50} value of 170 nM.

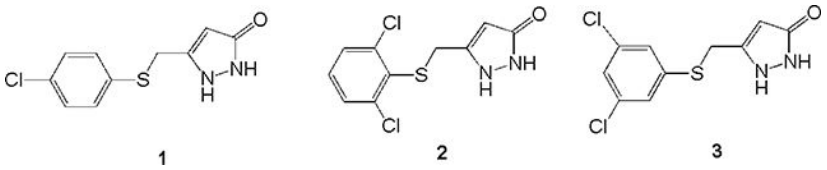

In vitro pharmacokinetic (PK) and *in vivo* brain/plasma ratio studies were also performed at an early stage of this drug development project. Other than having low microsomal stability and plasma stability, the ASP scaffold generally showed good PK properties and permeated the blood brain barrier.[21] Identifying and modifying the metabolic liability in the ASP scaffold, therefore, became a priority. The results of the metabolism studies, SAR investigations of the new scaffold, PK and toxicity properties, the ability to cross the blood-brain barrier, and effects on an ALS mouse model are described herein.

Results and Discussion

Chemistry

ASP analogs were synthesized as described earlier.[21] The syntheses of Type II ASP analogs with sulfoxide and sulfone linkers in place of the sulfide are shown in Scheme 1. The sulfide linker β-ketoester intermediates (**20–22)** were treated with $VO(acac)_2$-TBHP[22,23] to give the sulfoxide and sulfone intermediates (**23–26**) or with H_2O_2[24] to give sulfone **27**, which were treated with hydrazine to give the corresponding sulfoxide (**4,5**) and sulfone (**6-8**) products. The corresponding Type II aryloxanyl pyrazolone derivatives (**9-14**) were prepared from phenol and ethyl 4-chloroacetoacetate to generate the β-hydroxyester intermediates (**28-33**),[25] followed by treatment with hydrazine (Scheme 2). Although this two-step synthetic method is simple and direct, it is not efficient, mainly because of the low stability of the enolate derivatives from both the ethyl 4-chloroacetoacetate and the β-hydroxyester intermediates. Improved strategies to prepare the β-hydroxyester intermediates are described in Scheme 3. Compounds **42–47** were synthesized from the corresponding phenols and 2-bromo-*N*-methoxy-*N*-methylacetamide, which was obtained from 2-bromoacetyl bromide and *N,O*-dimethylhydroxylamine hydrochloride.[26] The corresponding β-hydroxyester intermediates were prepared by condensation of **42–47** with the enolate of ethyl acetate. The aryloxanyl pyrazolones (**13-19**) were obtained by treatment of the β-hydroxyester intermediates with hydrazine. Intermediates **39** and **41** were obtained via Suzuki coupling of aryl bromides **38** and **40**, respectively, with phenylboronic acid using a palladium catalyst.[27]

To avoid hydrolysis of Weinreb amide **36** under concentrated and strong basic conditions,[28,29] 3,5-dichlorophenol (**34**) was allowed to react with ethyl 2-bromoacetate then treated

with NaOH/H_2O to afford **35**. This intermediate was transformed to **42** with oxalyl chloride and *N,O*-dimethylhydroxylamine hydrochloride, and the Weinreb amide was converted to **13** as described above.

Microsomal Stability

ASP analogs, like 5-((2,4-dichloro-5-methylphenylthio)methyl)-1*H*-pyrazol-3(2*H*)-one (**48**, Figure 2) and 5-((4-chloro-2,5-dimethylphenylthio)methyl)-1*H*-pyrazol-3(2*H*)-one (**49**), were found to have low mouse liver microsomal stability. One possible site of metabolism by cytochrome P450 (CYP) isozymes[30] is the aromatic methyl group. Therefore, an analog lacking an aromatic methyl group **(1**) was tested for microsomal stability in the presence of NADPH, and the results were compared to minaprine (**50**), an antidepressant drug known to undergo rapid microsomal metabolism, as a positive control.[31] After incubation for 20 minutes with rat liver microsomes, minaprine and **1** were metabolized by 41% and 88%, respectively (Figure 3). Therefore, the aromatic methyl group is not responsible for the metabolic instability of **1**. Based on the above result, the most likely site of CYP metabolism is the sulfide sulfur atom, which is known to undergo oxidative metabolism.[32]

Metabolite Profiling of 1

Metabolic profiling was carried out on **1** despite its relatively low *in vitro* potency and because it contained a chlorine atom, which has a natural isotope abundance (^{35}Cl:^{37}Cl = 3:1) that can simplify the mass spectral analysis. The two likely metabolites are the corresponding sulfoxide (**4**) and sulfone (**6**), which were synthesized as shown in Scheme 1.

Compound **1** (15 μM) was incubated with rat liver microsomes at 37 °C for 0, 5, 10, 20, and 60 min in the presence of NADPH. HPLC analysis showed a new peak (5.90 min) that was not present prior to the addition of microsomes, and which was identified as the corresponding sulfoxide by comparison with those of synthetic standards of sulfoxide **4** (5.95 min) and sulfone **6** (10.8 min) (Figure 4).

Because of the limit of HPLC detection, the metabolite profiling of **1** was also carried out by LC/MS/MS. To assist in this analysis, an analog of **1** with ^{15}N substituted for both pyrazole nitrogens was synthesized by the route in Scheme 1 using $^{15}NH_2$-$^{15}NH_2$ in place of hydrazine. Both **1** and [$^{15}N_2$]-**1** (5 μM) were incubated with rat liver microsomes in the presence and absence of NADPH. After 0, 10, 20, 40, and 60 min, the samples were processed and analyzed by LC/MS/MS. Both compounds, in the presence of NADPH but not in its absence, produced one new peak not detected in the controls without microsomes or compound. The mass spectrum of the new peak corresponded to the sulfoxide (**4**). No sulfone was detected. The rate of formation of sulfoxide corresponded well with the loss of the sulfide (Figure 5).

Metabolism Guided Design and Synthesis of ASP Analogs

Because of the rapid metabolism of **1**, the sulfide was replaced by sulfoxide, sulfone, and ether functional groups, synthesized as shown in Schemes 1-3. These compounds were screened in the toxicity protection assay, and compounds that retained activity in this assay were tested for *in vitro* microsomal stability.

Mutant SOD1-induced Cytotoxicity Protection Assay of Modified Compounds

All of the ASP analogs exhibited 100% viability in the cytotoxicity protection assay, except for **4** (maximun viability ~ 35%). The EC_{50} values of these analogs in the protection assay are summarized in Table 1. In general, the potencies of the analogs were greater with the ether linkage, when compared with the sulfide, sulfone, and sulfoxide. The low sulfoxide potency indicated that metabolism of the ASPs to the corresponding sulfoxide results in deactivation of the compounds and that pursuing a prodrug strategy with the thioether linked compounds would not be possible. Therefore, a series of ether analogs, aryloxanyl pyrazolones, was synthesized (Table 1). Ether **13** (CMB-087229) was the most potent (67 nM) of these compounds. Analogs of **13**, having F, CF_3, Br, and Ph in place of the Cl atoms, indicated that size and electronics were important features at the meta-positions; the potency decreased in the following order: Cl > CF_3 > F > Br > Ph.

In Vitro ADME Assays

Microsomal Stability.—Human and mouse microsomal stabilities of sulfone **7** and ether analogs **9** and **13** were tested at 5 μM concentration at 37 °C for 1 h in the presence and absence of NADPH (Table 2). All three compounds showed good stability.

Aqueous Solubility.—The aqueous solubility of **7**, **9**, and **13** was evaluated by diluting them from a stock solution in DMSO to a final concentration of 1% DMSO in PBS (Table 3). The maximum solubility was considered to be the highest concentration that showed no precipitation. All three compounds showed good aqueous solubility.

Caco-2 Permeability.—Compounds **7**, **9**, and **13** all had high[33] permeability in the Caco-2 permeability assay (Table 4).

Protection of Primary Cortical Neurons.—It is not uncommon to observe that compounds that are active in tissue culture cells will not be active in differentiated neurons. Therefore sulfide **2**, sulfone **7**, and ether linker analog **13** were tested in a primary cortical neuron cell protection assay that showed all of these compounds were active. This issue was of particular concern because compounds from another scaffold, cyclohexane 1,3-diones, identified in the original high-throughput screen had poor activity in this assay, potentially due to poor cell permeability.[34]

PK Profiling of 13

Sulfone **7** and ether linker analogs **9** and **13** all showed good or adequate *in vitro* ADME properties. Compound **13** was selected based on its potency and *in vitro* pharmacological profile for *in vivo* PK profiling and efficacy in a mouse model of ALS.

Mouse *In Vivo* Steady-state Level and Blood-Brain Barrier Penetration for 13.—The *in vivo* steady-state level of ether analog **13** from plasma was determined in mice. The animals were administered 300 mg/kg **13** and sacrificed at progressive time points, (0, 3, 6, 12, and 24 h, Table 5), Blood and brain samples were harvested and analyzed by mass spectrometry using ESI ionization in the MRM mode.

***In Vivo* Rat PK Profiling of 13.—**Compound **13** was administered to Sprague-Dawley rats both intravenously and orally at 1 mg/kg in a single bolus dose. The results are summarized in Table 6.

Effect of 13 on the Potassium Channel.—The *in vitro* effect of **13** (10 μM) on the hERG potassium channel current expressed in human embryonic kidney cells (HEK293) was evaluated using a patch-clamp technique, the most definitive *in vitro* hERG inhibition assay.[35] A positive control (E-4031) was used to confirm the sensitivity of this test system, and the TurboSol evaluation system was performed on **13** to confirm that its insolubility was not a reason for low hERG inhibition observed in this test system (see Supporting Information for results). The mean % hERG antagonism (two experiments) was 0.6 ± 1.5%. These results indicate that **13** does not affect the hERG channel.

Effect of 13 on Cytochrome P450 Isozymes.—Compound **13** was tested for its inhibition CYP1A2, CYP2C9, CYP2C19, CYP2D6, and CYP3A4, present in human liver microsomes. IC_{50} values of **13** to CYP isozymes inhibition were evaluated using single drug substrates except for CYP3A4 (testosterone and midazolam tested). IC_{50} values were > 50 μM except for CYP2C19, which was 20 μM.

Effect of 13 on Enzymes and Receptors.—Compound **13** was screened at 10 μM concentration in duplicate by MDS Pharma Services (Taipei, Taiwan) with LeadProfilingScreen, a suite of 68 *in vitro* enzyme and receptor assays of the most commonly observed adverse CNS, cardiovascular, pulmonary, and genotoxic activities. No significant activity was detected in any of the 68 assays. See Supporting Information for results.

The Effect of 13 administration on SOD1 G93A ALS Mice.—Control and transgenic mice of the same age (± 3 days) and from the same “f” generation were selected from multiple litters to form experimental cohorts. The tolerable dose range for **13** was determined in wild type mice by increasing the dose b.i.d. one-fold each i.p. injection; the maximum tolerated dose was 75 mg/kg. Based on the studies performed to determine tolerance and blood brain levels, the dose levels of 1.0, 10, and 20 mg/kg once a day were administered, starting at 6 weeks of age, throughout the lives of the G93A mice. Administration of **13** resulted in a significant extension in survival in the G93A ALS mice in a dose dependent manner in comparison to untreated G93A mice (Figure 5). The most efficacious dose (20 mg/kg) resulted in a life extension of 13.3%.

Discussion

We had previously found that ASP compounds are metabolically unstable.[29] *In vitro* metabolic studies were carried out to determine the basis of microsomal instability. The early analogs had aromatic methyl groups (**48** and **49**) and a sulfide sulfur atom. Metabolic degradation of an ASP without an aromatic methyl (**1**) was more rapid than that of minaprine (**50**), a CNS drug known to undergo rapid metabolism, indicating that the instability was not caused by the aromatic methyl (Figure 3). Following microsome incubation, a new metabolite of **1** was identified by HPLC (Figure 4), which comigrated

with the corresponding sulfoxide (**4**); no sulfone (**6**) was detected. The formation of sulfoxide **4** quantitatively followed the degradation of **1** (Figure 5). The structure of the NADPH-dependent metabolite was further confirmed by LC/MS/MS; the NADPH dependence suggests that metabolism is catalyzed by a cytochrome P450.

Identification of the metabolite of **1** as the corresponding sulfoxide, which had poor activity in the cytotoxicity protection assay, guided our redesign of the arylsulfanyl pyrazolones to the corresponding sulfones and ethers (aryloxanyl pyrazolones). In general, the potency of compounds with the various linker groups increases (EC_{50} decreases) in the order ether > sulfide > sulfone >> sulfoxide.

A series of ether analogs was synthesized (Table 1) and all of the compounds were assayed in the cytotoxicity protection assay, which uses PC12 cells that express mutant G93A SOD1 as a YFP fusion protein.[20] In general, the most potent analogs were the 3,5-disubstituted phenyl analogs, where dichloro > dibromo > ditrifluoromethyl > difluoro > diphenyl. The dichloro analog (**13**) has an EC_{50} value of 67 nM.

Sulfone **7**, ether **9**, and ether **13** were much more metabolically stable than arylsulfanyl pyrazolone **1**,[29] with the ether being considerably more stable than the sulfone (Table 2). Because of the stability of the ethers, further ADME testing was carried out with the most potent analog (**13**).

The aqueous solubility of ether **13** was good (250 μM) as compared with that of **48** (56 μM[21]); although the solubility of sulfone **7** was greater than twice that of **13**. Permeability through Caco-2 monolayer cells correlates with *in vivo* intestinal permeability. The efflux of compounds in the opposite direction also can be estimated by this method. The high permeability values (P_{app} 27–43 × 10^{-6} cm/s) and low efflux ratios (P_{app} (B→A)/P_{app} (A→B); 0.2–0.6) of **7**, **9**, and **13** suggest that these compounds have high membrane permeability[36] and are likely poor substrates for efflux transport proteins, such as p-glycoprotein.[37]

To determine if these compounds are active in other types of cells, including neurons, a screen of selected compounds was carried out with four other cell types; SHSY-5Y, HeLa, HEK293, and primary cortical neuronal cells. Ether **13** was active in all four cell types, which is a positive indication of utility for the treatment of ALS, a non cell autonomous disease.[38]

Compound **13** was evaluated for its metabolic stability and blood-brain barrier penetration in mice. Mouse plasma stability was good, peaking at 3–6 hours; after 4 hours **13** was detected at 194 μM concentration in brain tissue. The loss of **13** does not follow first-order kinetics following intraperitoneal administration. Pharmacokinetics could be influenced by the high plasma protein binding by **13** (98% in rat and human), which can limit compound bioavailability in the plasma compartment, thereby prolonging the half-life.[39,40] However, high plasma protein binding alone does not determine the effect on the pharmacokinetic properties; the binding affinity (on/off rate) also is a major factor.[72] Pharmacokinetics in Sprague-Dawley rats was investigated both by i.v. and p.o. administration. The compound

appears to be reasonably stable and is orally active; half-lives were 2.1 and 3.6 hours, respectively, for these two routes of administration with oral bioavailability (%F) of 27%, which is above the typical cutoff for continued development of drug candidates[41] (Table 6). The difference in plasma stability from the mouse and rat studies could be the result of a combination of factors, including, different species (mouse vs. rat), different amount of compound used (5 mg/kg vs. 1 mg/kg), and route of administration (i.p. vs. i.v.).

Toxicity is an important cause for attrition of drug candidates at later stages of drug development. To reduce the time and effort of drug discovery, various toxicological criteria need to be met early on in the development of drug candidates. One is the effect of the compound on the human Ether-à-go-go Related Gene (hERG), a gene that encodes a cardiac potassium ion channel to regulate cardiac repolarization, which determines cardiac rhythmicity. When a compound inhibits the hERG ion channel, it can produce a disorder called long QT syndrome, resulting in torsade de pointes, heart arrhythmias and potentially sudden death. Therefore, it is essential that drug candidates do not affect hERG. Compound **13** did not antagonize hERG at a concentration of 10 μM.

The family of cytochrome P450 isozymes are also associated with drug toxicity.[42] Molecules that either inhibit or upregulate these enzymes can cause drug-drug interactions. If they inhibit the isozymes, metabolism of other drugs is blocked; if they upregulate the isozymes, it leads to rapid metabolism of drugs. The IC_{50} of compound **13** was > 50 μM for human liver CYP1A2, CYP2C19, CYP2D6, and CYP3A4 and 20 μM for CYP2C9, indicating that **13** should not cause drug-drug interactions.

To determine if there are other receptors or enzymes that might be potential off-targets, **13** was screened by MDS Pharma Services (Taipei, Taiwan) using its LeadProfilingScreen, a suite of 68 *in vitro* enzyme and receptor assays of the most commonly observed adverse CNS, cardiovascular, pulmonary, and genotoxic activities. Compound **13** showed no significant binding to any of these targets at 10 μM, suggesting that it is highly target selective.

Expression of genes with ALS-associated G93A SOD1 mutations produces a striking ALS phenotype motor neuron degeneration and paralysis in rats.[43,44] Transgenic mice that express human G93A mutant SOD1 develop hind limb weakness, muscle wasting, and neuropathological sequelae similar to those observed in both familial and sporadic ALS patients.[45] Candidate compounds are commonly tested in the ALS mouse model to evaluate their potential for the treatment of ALS.[13] The *in vivo* efficacy of riluzole, the only FDA-approved drug for ALS, was tested in G93A SOD1 mice and showed a lifespan extension of 7.5% when tested at 16 mg/kg[46] and of 11% at 22 mg/kg.[47] The *in vivo* efficacy of **13** in the mutant SOD1 G93A ALS mouse model was assessed to validate the aryloxanyl pyrazolone scaffold as a potential therapy for ALS,. Compound **13** produced a life extension of 13.3% at 20 mg/kg (Figure 6), comparable to or superior to riluzole.

Conclusions

We had previously identified arylsulfanyl pyrazolones (ASP) as a class of compounds exhibiting good potency against toxicity from protein aggregation by mutant SOD1.[21] These compounds could not be developed further, however, because of poor metabolic stability. Here we identify the cause for metabolic instability as the sulfide sulfur atom, which is oxygenated to the corresponding sulfoxide and show that the resulting sulfoxide compounds have significantly lower activity than the sulfides. Conversion to the corresponding sulfones and ethers, the aryloxanyl pyrazolones, resulted in much greater metabolic stability. The most potent analog was aryloxanyl pyrazolone **13**, with an IC_{50} of 67 nM, having good aqueous solubility, excellent Caco-2 permeability with low efflux potential, a rat plasma half-life of 3.6 h, rat oral bioavailability of 27%, neuron permeability, good mouse blood-brain barrier penetration (194 μM after 4 h), no effect on the hERG channel or 68 off-target proteins, and a life extension of G93A ALS mice of 13.3% at 20 mg/kg, as good or better than that previously reported for riluzole, the only FDA-approved therapeutic for ALS. These results support **13** as a novel drug candidate for the treatment of ALS.

Experimental Section

Chemistry. General methods, reagents and materials.

All reagents were purchased from Aldrich Chemical Co. (Milwaukee, WI) or Alfa Aesar (Ward Hill, MA) and were used without further purification, unless stated otherwise. Tetrahydrofuran was distilled under nitrogen from sodium/benzophenone. Dichloromethane was redistilled from CaH_2 under nitrogen. Other dry solvents were directly purchased. Thin-layer chromatography was carried out on E. Merck precoated silica gel 60 F_{254} plates. Compounds were visualized with ferric chloride reagent or a UV lamp. Column chromatography was performed with E. Merck silica gel 60 (230–400 mesh). Proton nuclear magnetic resonances (^{1}H NMR) were recorded in deuterated solvents on a Varian Inova 400 (400 MHz), a Varian Inova 500 (500 MHz) or a Bruker 500 (500 MHz) spectrometer. Chemical shifts are reported in parts per million (ppm, δ) using various solvents as internal standards ($CDCl_3$, δ 7.26 ppm; DMSO-d_6, δ 2.50 ppm). ^{1}H NMR splitting patterns are designated as singlet (s), doublet (d), triplet (t), or quartet (q). Splitting patterns that could not be interpreted or easily visualized were recorded as multiplet (m) or broad (br). Coupling constants are reported in Hertz (Hz). Proton-decoupled carbon (^{13}C NMR) spectra were recorded on a Varian Inova 500, a Varian Inova 400, or a Bruker 500 (125.7, 100.6, and 125.7 MHz, respectively) spectrometer and are reported in ppm using various solvents as internal standards ($CDCl_3$, δ 77.23 ppm; DMSO-d_6, δ 39.52 ppm). Electrospray mass spectra (ESMS) were obtained using an LCQ-Advantage spectrometer with methanol as the solvent in the positive ion mode. High-resolution mass spectra were carried out using a VG70–250SE mass spectrometer. Chemical ionization (CI) or electron impact (EI) was used as the ion source. Elemental analyses were performed by Atlantic Microlab Inc., Norcross, GA. All final compounds were analyzed for purity by HPLC using a Luna C18 (2) column (4.6 × 150, 5 μm; Phenomenex, Torrance, CA) at a flow rate of 1 mL/min with multiple HPLC conditions. Sample elution was detected by absorbance at 254 nm. HPLC was performed on a Beckman System Gold chromatograph (Model 125P solvent module and

Model 166 detector). All tested compounds had a purity of at least 95% as demonstrated by HPLC (see Supporting Information).

5-(4-Chlorophenylthio)-1*H*-[$^{15}N_2$]pyrazol-3(2*H*)-one (3).—4-Chlorothiophenol (1.1 g, 7.61 mmol) was mixed with ethyl 4-chloroacetoacetate (0.95 mL, 7.00 mmol) in CH_2Cl_2 (100 mL) at 0 °C. Triethylamine (1.5 mL, 10.8 mmol) was then added dropwise. After the resulting suspension was stirred at 0 °C for another 30 min, the reaction mixture was poured into water, and the aqueous layer was extracted with EtOAc. The combined organic layer was washed with saturated $NaHCO_3$, HCl (0.25 N), brine, concentrated in vacuo, and purified by flash column chromatography (ethyl acetate/hexanes = 1/9) to afford **20** (1.82 g) as a light yellow oil, which was not very stable. Therefore, **20** was used directly in the next step immediately after flash column chromatography purification. A proton NMR spectrum was taken immediately after the flash column purification. ^{1}H NMR (400 MHz, $CDCl_3$, δ): 7.37 (dd, *J* = 18.4, 8.4 Hz, 4H), 4.12 (d, *J* = 14.0, 7.2 Hz, 2H), 4.06 (s, 2H), 3.72 (s, 2H), 1.21 (t, *J* = 7.2 Hz, 3H). Compound **20** (0.52 g, 1.89 mmol) was stirred in EtOH (15 mL) and H_2O (6 mL), then $^{15}NH_2{}^{15}NH_2{\cdot}H_2SO_4$ (0.25 g, 1.89 mmol) and $NaHCO_3$ (0.32, 3.79 mmol) were added. The resulting solution was stirred overnight at room temperature, during which time a precipitate formed. The precipitate was filtered, washed with cold EtOH, and dried in vacuo to afford **3** (0.21 g, 44%, two steps) as a white solid. ^{1}H NMR (500 MHz, DMSO-d_6, δ): 11.48 (br s, 1H), 9.48 (br s, 1H), 7.36 (s, 4H), 5.30 (s, 1H), 4.08 (s, 2H); ^{13}C NMR (125 MHz, DMSO-d_6, δ): 161.3, 139.3, 135.0, 130.5, 129.8, 128.8, 89.6, 27.7; HRMS (m/z): [M + H]+ calcd for $C_{10}H_9Cl^{15}N_2OS$, 243.0142; found 243.0192.

5-(4-Chlorophenylsulfinyl)-1*H*-pyrazol-3(2*H*)-one (4).—Compound **20** was obtained from 4-chlorothiophenol and ethyl 4-chloroacetoacetate and used directly after flash column as described above. Compound **20** (1.27 g, 4.66 mmol) was mixed with *t*-butyl hydrogen peroxide (70 wt% in water, 1.1 mL, 7.69 mmol) in CH_2Cl_2 (50 mL) at room temperature, and vanadyl acetylacetonate (0.1% mol) was added slowly. Additional *t*-butyl hydrogen peroxide (0.5 mL, 3.50 mmol) was added to the reaction mixture after 2 h. The resulting suspension was stirred overnight at room temperature. The reaction mixture was then concentrated under vacuum and purified by flash column chromatography (ethyl acetate/hexanes = 1/4) to afford compound **23** (0.98 g) as a light yellow solid, which was not very stable. A proton NMR spectrum was taken immediately after the flash column purification. ^{1}H NMR (500 MHz, $CDCl_3$, δ): 7.46–7.34 (m, 4H), 4.20 (q, *J* = 7.5 Hz, 2H), 4.13 (s, 2H), 3.80 (s, 2H), 1.28 (t, *J* = 7.5 Hz, 3H). Therefore, **23** was used directly in the next step immediately after the flash column chromatography purification. Compound **23** (0.50 g, 1.73 mmol) was stirred in EtOH (6 mL), and an ethanolic solution of NH_2NH_2 (2 N, 0.87 mL, 1.74 mmol) was added. The resulting solution was stirred overnight at room temperature, during which time a precipitate formed. The precipitate was filtered, washed with cold EtOH, and dried in vacuo to afford **4** (0.10 g, 17%, three steps) as a white solid. ^{1}H NMR (500 MHz, DMSO-d_6, δ): 11.49 (br s, 1H), 9.75 (br s, 1H), 7.62 (d, *J* = 8.0 Hz, 2H), 7.54 (d, *J* = 9.0 Hz, 2H), 5.17 (s, 1H), 4.13–3.99 (m, 2H); ^{13}C NMR (125 MHz, DMSO-d_6, δ): 160.9, 142.5, 135.7, 132.1, 129.1, 126.3, 90.2, 53.3; HRMS (m/z): [M + H]+ calcd for $C_{10}H_9ClN_2O_2S$, 256.00733; found 256.00732.

5-(4-Chloro-2,5-dimethylphenylsulfinyl)-1*H*-pyrazol-3(2*H*)-one (5).—Analogous to **4**, compound **22** was prepared from 4-chloro-2,5-dimethylbenzenethiol (9 g, 52.1 mmol) to afford **22** (13.11 g). Immediately after flash chromatography, **22** (4.69 g, 14.2 mmol) was converted to **24** (3.20 g). Immediately after flash column chromatography, **24** (1.39 g, 4.00 mmol) was converted to **5** as a white solid (0.42 g, 19%, three steps). ^{1}H NMR (500 MHz, DMSO-d_6, δ): 11.52 (br s, 1H), 9.50 (br s, 1H), 7.58 (s, 1H), 7.37 (s, 1H), 5.22 (s, 1H), 4.03–3.93 (m, 2H), 2.35 (s, 3H), 2.15 (s, 3H); ^{13}C NMR (125 MHz, DMSO-d_6, δ): 161.1, 140.8, 135.7, 134.7, 134.1, 132.5, 130.3, 126.1, 90.9, 52.3, 19.3, 16.8.

5-(4-Chlorophenylsulfonyl)-1*H*-pyrazol-3(2*H*)-one (6).—Compound **20** was obtained from 4-chlorothiophenol and ethyl 4-chloroacetoacetate and used directly after flash column as described above. Compound **20** (3.0 g, 11.0 mmol) was mixed with *t*-butyl hydrogen peroxide (70 wt% in water, 1.5 mL, 10.5 mmol) in CH_2Cl_2 (50 mL) at room temperature, and vanadyl acetylacetonate (0.1% mol) was added slowly. Additional *t*-butyl hydrogen peroxide (6 mL, 41. 94 mmol) was added to the reaction mixture gradually until all starting material was consumed, as determined by TLC. The resulting suspension was stirred overnight at room temperature. The reaction mixture was then concentrated under vacuum and purified by flash column chromatography (ethyl acetate/hexanes = 1/4) to afford **25** (1.61 g) as a light yellow oil, which was not very stable. Therefore, **25** was used directly in the next step immediately after flash column chromatography purification. Compound **25** (1.60 g, 5.25 mmol) was stirred in EtOH (6 mL), and an ethanolic solution of NH_2NH_2 (2 N, 2.64 mL, 5.28 mmol) was added. The resulting solution was stirred overnight at room temperature, during which time a precipitate formed. The precipitate was filtered, washed with cold EtOH, and dried under vacuum to afford **6** (0.46 g, 12%, three steps) as a white solid. ^{1}H NMR (500 MHz, DMSO-d_6, δ): 11.24 (br s, 1H), 7.75 (d, J = 9.0 Hz, 2H), 7.67 (d, J = 8.5 Hz, 2H), 5.21 (s, 1H), 4.56 (s, 2H); ^{13}C NMR (125 MHz, DMSO-d_6, δ): 159.1, 139.0, 137.2, 130.1, 129.4, 89.9, 54.1; HRMS (m/z): [M + H]+ calcd for $C_{10}H_9ClN_2O_3S$, 272.00224; found 272.00164.

5-(3,5-Dichlorophenylsulfonyl)-1*H*-pyrazol-3(2*H*)-one (7).—Analogous to **6**, compound **21** (4.20 g) was prepared from 3,5-dichlorobenzenethiol (2.5 g, 14.0 mmol). Immediately after flash chromatography, **21** (4.10 g, 13.3 mmol) was converted to **26** (2.24 g). Immediately after flash chromatography, **26** (2.14 g, 6.31 mmol) was converted to **7** as a white solid (0.38 g, 10%, three steps). ^{1}H NMR (500 MHz, DMSO-d_6, δ): 11.62 (br s, 1H), 9.55 (br s, 1H), 7.77–7.36 (m, 3H), 5.26 (s, 1H), 4.70 (s, 2H); ^{13}C NMR (125 MHz, DMSO-d_6, δ): 161.3, 141.2, 135.0, 133.8, 129.5, 126.7, 92.1, 52.5; HRMS (m/z): [M + H]+ calcd for $C_{10}H_8Cl_2N_2O_3S$, 301.0408; found 301.0415.

5-(4-Chloro-2,5-dimethylphenylsulfonyl)-1*H*-pyrazol-3(2*H*)-one (8).—Compound **22** was obtained from 4-chloro-2,5-dimethylbenzenethiol and ethyl 4-chloroacetoacetate and used directly after flash column chromatography as described above. Compound **22** (4.68 g, 14.1 mmol) was mixed with AcOH (5 mL) in EtOAc (10 mL), and H_2O_2 (30 % in water, 10 mL, 84.6 mmol) was added. The resulting solution was left stirring at room temperature overnight after which additional H_2O_2 (30 % in water, 5 mL, 42.3 mmol) was added. The reaction mixture was then evaporated under vacuum and purified by flash column

chromatography (ethyl acetate/hexanes = 1/3) to afford **27** (4.34 g) as a yellowish oil, which was not very stable. Therefore, **27** was used directly in the next step immediately after flash column chromatography purification. Compound **27** (4.33 g, 11.9 mmol) was stirred in EtOH (20 mL), and an ethanolic solution of NH_2NH_2 (2 N, 5.98 mL, 11.9 mmol) was added. The resulting solution was stirred overnight at room temperature, during which time a precipitate formed. The precipitate was filtered, washed with cold EtOH, and dried under vacuum to afford **8** (0.71 g, 17%, three steps) as a white solid. ^{1}H NMR (500 MHz, DMSO-d_6, δ): 11.62 (br s, 1H), 9.59 (br s, 1H), 7.67 (s, 1H), 7.54 (s, 1H), 5.24 (s, 1H), 4.49 (s, 2H), 2.47 (s, 3H), 2.33 (s, 3H); ^{13}C NMR (125 MHz, DMSO-d_6, δ): 160.3, 138.8, 137.7, 135.2, 133.9, 132.5,132.4, 131.0, 91.8, 53.1, 43.3, 19.1; HRMS (m/z): [M + H]+ calcd for $C_{12}H_{13}ClN_2O_3S$, 306.9705; found 306.9713.

Synthesis of ether analogs (9–13) via method A.

5-((4-Chlorophenoxy)methyl)-1*H*-pyrazol-3(2*H*)-one (9).—A solution of 4-chlorophenol (6.4 g, 50 mmol) in THF (25 mL) was treated with NaH (60% in mineral oil, 2 g, 50 mmol) at 0 °C. In another flask, a solution of ethyl 4-chloroacetoacetate (10.21 mL, 75 mmol) in THF (25 mL) was treated with NaH (60% in mineral oil, 3.5 g, 75 mmol) at −20 °C. The resulting yellowish suspension was slowly added to the solution of sodium 4-chlorophenoxide, which was kept at 0 °C. After the addition of DMF (10 mL), the reaction temperature was slowly raised to 70 °C. After the reaction mixture was stirred at 70 °C overnight, it was cooled and evaporated to dryness. The residue was purified by flash column chromatography (ethyl acetate/hexanes = 1/9) to afford **28** (10.7 g, contains 30% 4-chloroacetonacetate) as a yellowish oil. The obtained mixture was used directly in the next step. To the mixture of **28** and 4-chlorophenol (10.7 g, assumed 41.7 mmol) was added an ethanolic solution of NH_2NH_2 (2 N, 14.5 mL, 29.0 mmol). The resulting solution was stirred overnight at room temperature, during which time a precipitate formed. The precipitate was filtered, washed with cold EtOH, and dried under vacuum to afford **9** (1.38 g, 13%, two steps) as a white solid. ^{1}H NMR (500 MHz, DMSO-d_6, δ): 11.79 (br s, 1H), 9.56 (br s, 1H), 7.33 (d, J = 9.0 Hz, 2H), 7.02 (d, J = 9.0 Hz, 2H), 5.52 (s, 1H), 4.92 (s, 2H); ^{13}C NMR (125 MHz, DMSO-d_6, δ): 160.2, 157.0, 139.2, 129.3, 124.6, 116.6,89.5, 62.1.

5-((4-Ethylphenoxy)methyl)-1*H*-pyrazol-3(2*H*)-one (10).—Analogous to **9**, compound **29** was prepared from 4-ethylphenol (3.0 g, 24.6 mmol). The mixture of **29** and 4-ethylphenol (4.05 g, assumed 16.2 mmol) was converted to **10** (1.62 g, 30%, two steps) as a white solid. ^{1}H NMR (500 MHz, DMSO-d_6, δ): 11.75 (br s, 1H), 9.50 (br s, 1H), 7.10 (d, J = 8.0 Hz, 2H), 6.89 (d, J = 8.5 Hz, 2H), 5.50 (s, 1H), 4.87 (s, 2H), 2.54–2.51 (m, 2H), 1.13 (t, J = 7.5 Hz, 3H); ^{13}C NMR (125 MHz, DMSO-d_6, δ): 160.0, 156.2, 140.3, 136.1, 128.7, 114.6, 89.4, 61.6, 27.4, 16.0.

5-((3-Ethylphenoxy)methyl)-1*H*-pyrazol-3(2*H*)-one (11).—Analogous to **9**, compound **30** was prepared via method A from 3-ethylphenol (3.0 g, 24.6 mmol). The mixture of **30** and 3-ethylphenol (1.81 g, assumed 7.23 mmol) was converted to **10** (0.30 g, 6%, two steps) as a white solid. ^{1}H NMR (500 MHz, DMSO-d_6, δ): 11.79 (br s, 1H), 9.55 (br s, 1H), 7.18 (t, J = 7.8 Hz, 1H), 6.83–6.79 (m, 3H), 5.52 (s, 1H), 4.89 (s, 2H), 2.56 (q, J =

7.5 Hz, 2H), 1.16 (t, J = 7.5 Hz, 3H); ^{13}C NMR (125 MHz, DMSO-d_6, δ): 160.7, 158.2, 145.4, 139.3, 129.3,120.4, 114.3, 111.8, 89.8, 61.0, 28.3, 15.6.

5-((3-*tert*-Butylphenoxy)methyl)-1*H*-pyrazol-3(2*H*)-one (12).—Analogous to **9**, compound **31** was prepared via method A from 3-*tert*-butylphenol (3.0 g, 20.0 mmol). The mixture of **31** and 3-*tert*-butylphenol (2.47 g, assumed 8.86 mmol) was treated with NH_2NH_2 (2 N, 4.40 mL, 8.80 mmol) to give **10** (1.52 g, 10%, two steps) as a white solid. ^{1}H NMR (500 MHz, DMSO-d_6, δ): 11.72 (br s, 1H), 9.50 (br s, 1H), 7.20 (t, J = 8.0 Hz, 1H), 6.97–6.80 (m, 3H), 5.52 (s, 1H), 4.91 (s, 2H); ^{13}C NMR (125 MHz, DMSO-d_6, δ): 160.7, 157.9, 152.4, 138.7, 129.0, 117.8, 112.3, 111.1, 89.7, 61.0, 34.5, 31.3.

5-((3,5-Dichlorophenoxy)methyl)-1*H*-pyrazol-3(2*H*)-one (13).—Analogous to **9**, compound **32** was prepared via method A from 3,5-dichlorophenol (2.0 g, 12.3 mmol). The mixture of **32** and 3,5-dichlorophenol (1.10 g, assumed 3.78 mmol) was treated with NH_2NH_2 (2 N, 1.90 mL, 3.80 mmol) to give **13** (66.1 mg, 2%, two steps) as a white solid. See below (Method B) for characterization of **13**.

5-((3,5-Bis(trifluoromethyl)phenoxy)methyl)-1*H*-pyrazol-3(2*H*)-one (14).—Analogous to **9**, compound **33** was prepared via method A from 3,5-bis(trifluoromethyl)phenol (1.00 mL, 5.93 mmol). The mixture of **33** and 3,5-bis(trifluoromethyl)phenol (0.72 g, assumed 2.00 mmol) was treated with NH_2NH_2 (2 N, 1.00 mL, 2.00 mmol) to give **14** (0.40 g, 20%, two steps) as a white solid. ^{1}H NMR (500 MHz, DMSO-d_6, δ): 11.62 (br s, 1H), 9.50 (br s, 1H), 7.99 (s, 2H), 7.86 (s, 1H), 5.35 (s, 1H), 4.31 (s, 2H); ^{13}C NMR (125 MHz, DMSO-d_6, δ): 159.8, 140.9, 131.2, 130.9, 130.5, 130.2, 127.6, 127.2, 124.5, 121.8, 119.1, 118.8, 89.0, 27.6.

Synthesis of ether analogs (13, 15–19) via method B.

Detailed experimental procedures and characterization of **35**, **36**, **39**, **41**, and **42–47** can be found in the Supporting Information.

5-((3,5-Dichlorophenoxy)methyl)-1*H*-pyrazol-3(2*H*)-one (13).—EtOAc (3.20 mL. 32.7 mmol) was added to a solution of LiHMDS (1 N in THF, 75.0 mL, 75.0 mmol) at 0 °C and stirred. After 60 min, a THF solution of **42** (8.55 g, 32.4 mmol) was added dropwise at −78 °C. After the resulting solution was stirred at −78 °C for another 8 h, the reaction mixture was quenched with diluted HCl (0.25 N), the pH was adjusted to 3–5, and the aqueous layer was extracted with Et_2O. The combined organic layer was dried over Na_2SO_4 and concentrated under vacuum. The residue was purified by flash column chromatography (ethyl acetate/hexanes = 1/9) to give ethyl 4-(3,5-dichlorophenoxy)-3-oxobutanoate (3.28 g) as a white solid. The proton NMR spectrum was taken immediately after recrystallization (ethyl acetate/hexanes). ^{1}H NMR (500 MHz, $CDCl_3$, δ): 7.02 (t, J = 1.7 Hz, 1H), 6.81 (d, J = 1.7 Hz, 2H), 4.68 (s, 2H), 4.21 (q, J = 7 Hz, 2H), 3.61 (s, 2H), 1.28 (t, J = 7 Hz). Ethyl 4-(3,5-dichlorophenoxy)-3-oxobutanoate was used directly in the next step immediately after the flash column chromatography purification. Ethanolic hydrazine (2 N, 5.60 mL, 11.2 mmol) was added to a solution of ethyl 4-(3,5-dichlorophenoxy)-3-oxobutanoate (3.28 g, 11.3 mmol) in EtOH (25 mL). The resulting solution was stirred at room temperature

overnight. The reaction mixture was then evaporated under vacuum, purified by flash column chromatography (ethyl acetate/hexanes = 1/2) and recrystallized in ethyl acetate/hexanes to give **13** (0.88 g, 11%, two steps) as white crystals. ^{1}H NMR (500 MHz, DMSO-d_6, δ): 11.82 (br s, 1H), 9.54 (br s, 1H), 7.16 (s, 1H), 7.12 (d, *J* = 1.5 Hz, 2H), 5.53 (s, 1H), 4.99 (s, 2H); ^{13}C NMR (125 MHz, DMSO-d_6, δ): 161.0, 159.4, 137.8, 134.6, 120.6, 114.2, 90.7, 61.5. Anal. Calcd for $C_{10}H_8Cl_2N_2O_2$: C, 46.36; H, 3.11; Cl, 27.37; N, 10.81. Found: C, 46.40; H, 3.08; Cl, 27.24; N, 10.65. All values are given as percentages.

5-((3,5-Difluorophenoxy)methyl)-1*H*-pyrazol-3(2*H*)-one (15).—Analogous to **13**, compound **15** was prepared via method B from **43** (1.24 g, 5.36 mmol) to afford initially ethyl 4-(3,5-difluorophenoxy)-3-oxobutanoate (0.89 g, 3.44 mmol). Because of instability, immediately after flash column chromatography, ethyl 4-(3,5-difluorophenoxy)-3-oxobutanoate (0.89 g, 3.44 mmol) was treated with NH_2NH_2 (2 N in EtOH, 1.70 mL, 3.40 mmol) to give **15** as a white solid (50.9 mg, 5%, two steps). ^{1}H NMR (500 MHz, DMSO-d_6, δ): 11.82 (br s, 1H), 9.53 (br s, 1H), 6.80–6.79 (m, 3H), 5.56 (s, 1H), 4.95 (s, 2H); ^{13}C NMR (125 MHz, DMSO-d_6, δ): .1, 164.0, 162.1, 162.0, 160.0, 146.4, 137.8, 99.1, 98.9, 96.4, 90.7, 61.8.

5-((3,5-Dibromophenoxy)methyl)-1*H*-pyrazol-3(2*H*)-one (16).—Analogous to **13**, compound **16** was prepared via method B from **44** (1.07 g, 3.03 mmol) to afford initially ethyl 4-(3,5-dibromophenoxy)-3-oxobutanoate (0.35 g). Immediately after flash column, ethyl 4-(3,5-dibromophenoxy)-3-oxobutanoate (0.35 g, 0.92 mmol) was treated with NH_2NH_2 (2 N in EtOH, 0.46 mL, 0.92 mmol) to give **16** as a white solid (23.7 mg, 2%, two steps). ^{1}H NMR (500 MHz, DMSO-d_6, δ): 11.80 (br s, 1H), 9.52 (br s, 1H), 7.39 (s, 1H), 7.28 (m, 2H), 5.55 (s, 1H), 4.99 (s, 1H); ^{13}C NMR (125 MHz, DMSO-d_6, δ): 161.0, 159.5, 137.7, 125.9, 122.8, 117.4, 90.6, 61.5.

5-((3-Bromophenoxy)methyl)-1*H*-pyrazol-3(2*H*)-one (17).—Analogous to **13**, compound **17** was prepared via method B from **45** (2.43 g, 8.87 mmol) to afford initially ethyl 4-(3-bromophenoxy)-3-oxobutanoate (1.07 g). Immediately after flash column, ethyl 4-(3-bromophenoxy)-3-oxobutanoate (1.07 g, 3.55 mmol) was treated with NH_2NH_2 (2 N in EtOH, 1.70 mL, 3.40 mmol) to give **17** as a white solid (0.42 g, 18%, two steps). ^{1}H NMR (500 MHz, DMSO-d_6, δ): 11.78 (br s, 1H), 9.50 (br s, 1H), 7.26–7.23 (m, 1H), 7.14–7.13 (m, 1H), 7.02–7.00 (m, 2H), 5.58 (s, 1H), 4.96 (s, 2H); ^{13}C NMR (125 MHz, DMSO-d_6, δ): 161.6, 159.1, 138.4, 131.2, 123.8, 122.1, 117.6, 114.3, 90.5, 61.3.

5-((Biphenyl-3-yloxy)methyl)-1*H*-pyrazol-3(2*H*)-one (18).—Analogous to **13**, compound **18** was prepared via method B from **46** (0–.74 g, 2.74 mmol) to afford initially ethyl 4-(biphenyl-3-yloxy)-3-oxobutanoate (0.50 g). Immediately after flash column, ethyl 4-(biphenyl-3-yloxy)-3-oxobutanoate (0.50 g, 1.68 mmol) was treated with NH_2NH_2 (2 N in EtOH, 0.84 mL, 1.68 mmol) to give **18** as a white solid (0.19 g, 27%, two steps). ^{1}H NMR (500 MHz, DMSO-d_6, δ): 11.80 (br s, 1H), 9.50 (br s, 1H), 7.67–6.99 (m, 9H), 5.55 (s, 1H), 5.02 (s, 2H); ^{13}C NMR (125 MHz, DMSO-d_6, δ): 161.3, 158.6, 138.7, 141.7, 140.0, 130.0, 128.9, 127.7, 126.8, 119.4, 113.9, 113.0, 90.3, 60.8.

5-((5-Phenylbiphenyl-3-yloxy)methyl)-1*H*-pyrazol-3(2*H*)-one (19).—Analogous to **13**, compound **19** as prepared via method B from **47** (0.61 g, 1.75 mmol) to afford initially ethyl 4-(5-phenylbiphenyl-3-yloxy)-3-oxobutanoate (0.45 g). Immediately after flash column, ethyl 4-(5-phenylbiphenyl-3-yloxy)-3-oxobutanoate (0.45 g, 1.21 mmol) was treated with NH_2NH_2 (2 N in EtOH, 0.60 mL, 1.20 mmol) to give **19** as a white solid (0.19 g, 27%, two steps). ^{1}H NMR (500 MHz, DMSO-d_6, δ): 11.82 (br s, 1H), 9.50 (br s, 1H), 7.76 (d, *J* = 8.0 Hz, 4H), 7.50–7.38 (m, 7H), 7.27 (s, 2H), 5.60 (s, 1H), 5.13 (s, 2H); ^{13}C NMR (125 MHz, DMSO-d_6, δ): 161.3, 159.1, 142.3, 140.0, 139.0, 129.0, 127.8, 127.0, 118.0, 112.3, 90.4, 61.2.

In Vitro Microsomal Stability of Compound 1 and Minaprine. General methods, reagents and materials.

The microsome assay was measured on a Beckman HPLC system using Luna C18 (2) column (4.6 × 150, 5 μm; Phenomenex, Torrance, CA) at a flow rate of 1 mL/min at 254 nm for minaprine and 260 nm for **1**. Solid phase extraction was carried out using Waters Sep-Pak®Vac C18 1 cc cartridges (Waters Chromatography, Milford, MA). NADPH regeneration solutions and rat liver microsomes were purchased from Bectin-Dickinson.

To PBS (10 mL) was added NADPH regeneration buffer A (500 μL) and NADPH regeneration buffer B (100 μL) to make the PBS+ solution. To the PBS+ solution (255 μL) was added the compound of interest (30 μL of 150 μM stock in PBS+) in an Eppendorf tube. Each reaction mixture was carried out in PBS (pH 7.4), which contained 1 mg/mL microsomal protein with 1.3 mM $NADP^+$, 3.3 mM glucose-6-phosphate, 0.4 U/mL glucose-6-phosphate dehydrogenase, and 3.3 mM magnesium chloride. The tubes were vortexed and equilibrated at 37 °C. The samples were incubated at 37 °C for 0 and 20 min after the rat liver microsomes (15 μM) were added. Acetonitrile (40 μL) and haloperidol (internal standard; 100 μL) were added as a quench solution. The reaction mixture was vortexed and left in a −78 °C ice bath immediately after it was quenched. The samples were centrifuged (13.4 krpm, 12 min), and the supernatant was loaded onto a Waters Sep-Pak®Vac C18 1 cc SPE cartridge. The loaded SPE column was washed with H_2O (2 × 1 mL), and the compounds were eluted with acetonitrile/H_2O = 1/1 (2 × 1 mL). The solvent was removed under vacuum. The samples were reconstituted in DMSO/H_2O = 1/9 (25 μL), and an aliquot (20 μL) was analyzed by HPLC (isocratic; acetonitrile/H_2O = 25/75, 60 min; 0.1% TFA). The response ratio (RR) was calculated by dividing the peak area of the analyte by the peak area of the internal standard. Peak integrals were normalized by dividing by the area for the peak at t = 0 min. Sample HPLC spectrum and RR data can be found in the Supporting Information.

Metabolite Profiling of Compound 1.

Compound **1** was incubated with rat liver microsomes and NADPH regeneration buffers as described above for the in vitro microsomal stability study of **1**. To the PBS+ solution (85 μL) was added **1** (10 μL of 150 μM stock in PBS+). The sample was incubated at 37 °C for 0, 5, 10, 20, 40, and 60 min after the rat liver microsomes (15 μM) were added. Acetonitrile (50 μL) was added as a stop solution. The reaction was vortexed and left on a −78 °C ice bath immediately after it was quenched. The samples were centrifuged (13.4 krpm, 12 min),

and the supernatant (20 μL) was directly analyzed by HPLC (isocratic; acetonitrile/H_2O = 25/75, 30 min; 0.1% TFA). Compounds **4** (20 μL, 10 μM) and **6** (20 μL, 10 μM) were analyzed by the same HPLC program. Spectra of the microsomal incubation residue of **1**, standard solution of **4**, and standard solution of **6** were compared in parallel.

Further metabolite profiling of 1 and 3.

Metabolite studies were also performed at Apredica, Inc. (Watertown, MA). Samples were analyzed by LC/MS/MS using either an Agilent 6410 mass spectrometer coupled with an Agilent 1200 HPLC and a CTC PAL chilled autosampler or an ABI2000 mass spectrometer coupled with an Agilent 1100 HPLC and a CTC PAL chilled autosampler. After separation of compounds on a C18 reverse phase HPLC column using an acetonitrile-water gradient system, peaks were analyzed by mass spectrometry using ESI ionization in MRM mode.

Each test agent (**1** and **3**) was incubated in duplicate at 5 μM with or without rat liver microsomes in the presence and absence of NADPH. After 0, 10, 20, 40, and 60 min incubation, an aliquot was removed from each reaction, the protein was precipitated with acetonitrile containing internal standard. The supernatant was analyzed by LC/MS/MS. Detailed experimental data, HPLC, and MS spectra can be found in the Supporting Information.

Mutant SOD1-induced Cytotoxicity Protection Assay.

Viability and EC_{50} values of **1**-**19** were determined according to the previously reported assay procedure.[20] PC12 cells expressing mutant G93A SOD1 were seeded at 15000 cells/well in 96-well plates and incubated fro 24 h prior to compound addition. Compounds were assayed in 12-point dose-response experiments to determine potency and efficacy. The highest compound concentration tested was 32 μM, which was decreased by one-half with each subsequent dose. After 24 h incubation with the compounds, MG132 was added at a final concentration of 100 nM. MG132 is a well-characterized proteasome inhibitor, which enhances the appearance of protein aggregation by blocking the proteosomal clearance of aggregated proteins. Cell viability was measured 48 h later using a fluorescent viability probe, Calcein-AM (Molecular Probes). Briefly, cells were washed twice with PBS, Calcein-AM was added at a final concentration of 1 μM for 20 min at room temperature, and fluorescence intensity was read in a POLARstar fluorescence plate reader (BMG). Fluorescence data were coupled with compound structural data, then stored, and analyzed using the CambridgeSoft Chemoffice Enterprise Ultra software package.

In Vitro ADME Assays.

In vitro microsomal stability of **7** and **9**, aqueous solubility, and Caco-2 permeability of **7**, **9**, and **13** were determined according to the previously reported procedure.[21] *In vitro* microsomal stability of **13** was obtained from Biogen Idec.

Preliminary Cortical Neuron Permeability.

Primary rat cortical tissue was purchased from Neuromics Inc., Edina, MN and used to initiate primary cortical neuron cultures. The tissue was isolated from micro-surgically

dissected E18 embryonic Sprague-Dawley or Fischer 344 rat brain and shipped in a nutrient rich medium under refrigeration.

To isolate neurons, the tissue was incubated with papain at a concentration of 2 mg/mL in Hibernate without calcium for 30 min at 37 °C. The enzymatic solution was then removed and 1 mL of culture media (Neurobasal, B27, 0.5 mM glutamine) was added. A sterile Pasteur pipette was used to gently disperse the cells, which were then washed, re-suspended and counted. The cells were plated on poly-D-lysine coated 96-well plates at a density of 20,000 cells/well and incubated at 37 °C in a 5% CO_2-humidified atmosphere for 5 days prior to use in compound testing. By microscopic inspection, the resulting culture consisted of ~90% neurons.

Test compounds were assayed in six-point dose response experiments. The highest compound concentration tested was 100 μM, which was then diluted by approximately one-third with each subsequent dose. After 24 h incubation with the compounds, MG132 was added at a final concentration of 100 nM, a dose that produces an approximately 70% loss of viability. Cell viability was measured 48 h later using the fluorescent viability probe, Calcein-AM (Molecular Probes, Invitrogen, Carlesbad, CA). Briefly, cells were washed twice with PBS, Calcein-AM was added at a final concentration of 1 μM for 20 min at room temperature, and fluorescence intensity was then read in a POLARstar fluorescence plate reader (BMG). Compounds that restored viability at any dose to a level equal or higher than 5 standard deviations from MG132 controls were considered active.

In Vivo Mouse Drug Steady-State Level Determination and in Vivo Brain Penetration.

See Supporting Information.

In Vivo PK Profiling

In vivo PK profiling was performed by administering a 300 mg/kg bolus intraperitoneal injection of **13** into B6SJL mice. Blood and brain samples were collected at 0, 1, 3, 6, 12, and 24 h time points and flash frozen in liquid nitrogen, stored at −80 °C, and shipped to Apredica, Inc. for analysis. The analysis was carried out as for for *in vivo* mouse drug steady-state level determination and *in vivo* brain penetration described in Supporting Information.

Effect of Compound 13 on Potassium Channels

FASTPatch hERG screen assay, using cloned hERG potassium channels expressed in human embryonic kidney cells (HEK293), was carried out by ChanTest Corporation (Cleveland, OH).

In Vivo SOD1 G93A ALS Mice Study of 13.

G93A SOD1 mice and littermate SOD1 mice were mated with B6SJL females, and the offspring were genotyped by PCR using tails. A 12-h light-dark cycle was maintained, and animals were given free access to food and water. Control and transgenic mice of the same age (± 3 days) and from the same “f” generation were selected from multiple litters to form experimental cohorts (n = 20 per group). Standardized criteria for age, weight, and parentage

were used for placing individual mice into experimental groups/cohorts. Wild type mice were used for initial toxicity, tolerability, and pharmacokinetics studies. The tolerable dose range and LD50 for **13** was determined in the wild type mice by increasing the dose b.i.d. one-fold each injection and observed at 75 mg/kg. Drug steady-state level was determined in animals that had been dosed for one week prior to sacrifice. The dosing levels of 1.0, 10, and 20 mg/kg once a day were administered throughout the levels of the G93A mice.

Efficacy was measured using endpoints that clearly indicate neuroprotective function. These include amelioration of degenerative changes in the spinal cord, improved motor function, and prolonged survival. The mice cohorts were sacrificed at end stage disease using criteria for euthanasia, followed temporally for survival analyses. Mice were observed three times daily (morning, noon, and later afternoon) throughout the experiment. Mice were euthanized when disease progression was sufficiently severe that they were unable to initiate movement and right themselves after gentle prodding for 30 seconds.

Data sets were generated and analyzed for each clinical and neuropathological measure. Effects on behavior and neuropathology were compared in treatment and control groups. Dose-dependent effects were assessed in each treatment group using multiple two-sided ANOVA testes. Multiple comparisons in the same subject groups were dealt with post hoc. Kaplan-Meier analysis was used for survival function. All other statistical analyses were performed using Student's t-test. Data are expressed as the mean ± SEM. Statistical comparisons of histological data were made by ANOVA.

Supplementary Material

Refer to Web version on PubMed Central for supplementary material.

Acknowledgements.

We thank the National Institutes of Health [1R43NS057849], the ALS Association (TREAT program), the Department of Defense [AL093052] and the Center for ALS Research at the Univesity of Pittsburgh for their generous support of the research project. The authors are grateful to Biogen Idec Inc. for carrying out the *in vivo* rat PK profiling tests, in vitro P450 reversible inhibition study, the plasma binding affinity assay, the hERG inhibition assays; and MDS Pharma Service (now Ricerca Biosciences, LLC) for carrying out the LeadProfilingScreen of **13**.

a Abbreviations:

ADME	absorption, distribution, metabolism, and excretion
ALS	amyotrophic lateral sclerosis
ASP	arylsulfanyl pyrazolone
CYP	cytochrome P450
FALS	familial amyotrophic lateral sclerosis
HEK	human embryonic kidney
hERG	human Ether-à-go-go-Related Gene

HTS	high-throughput screen
MRM	multiple reaction monitoring
PK	pharmacokinetics
SOD1	Cu/Zn superoxide dismutase 1
SALS	sporadic amyotrophic lateral sclerosis

References

1. Bruijn LI; Miller TM; Cleveland DW Unraveling the mechanisms involved in motor neuron degeneration in ALS. Annu. Rev. Neurosci 2004, 27, 723–749. [PubMed: 15217349]
2. Hirtz D; Thurman DJ; Gwinn-Hardy K; Mohamed M; Chaudhuri AR; Zalutsky R How common are the “common” neurologic disorders. Neurology 2007, 68, 326–337. [PubMed: 17261678]
3. Cronin S; Hardiman O; Traynor BJ Ethnic variation in the incidence of ALS. Neurology 2007, 68, 1002–1007. [PubMed: 17389304]
4. Haley RW Excess incidence of ALS in young Gulf War veterans, Neurology 2003, 61, 750–756. [PubMed: 14504316]
5. Horner RD; Kamins KG; Feussner JR; Grambow SC; Hoff-Lindquist J; Harati Y; Mitsumoto H; Pascuzzi R; Spencer PS; Tim R; Howard D; Smith TC; Ryan MAK; Coffman CJ; Kasarskis EJ Occurrence of amyotrophic lateral sclerosis among Gulf War veterans. Neurology 2003, 61, 742–749. [PubMed: 14504315]
6. Weisskopf MG; O’Reilly EJ; McCullough ML; Calle EE; Thun MJ; Cudkowicz M; Ascherio A Prospective study of military service and mortality from ALS. Neurology 2005, 64, 32–37. [PubMed: 15642900]
7. Rowland LP; Shneider NA Amyotrophic lateral sclerosis. N. Engl. J. Med 2001, 344, 1688–1700. [PubMed: 11386269]
8. Miller RG; Mitchell JD; Moore DH Riluzole for amyotrophic lateral sclerosis (ALS)/motor neuron disease (MND). Amyotroph. Lat. Scler. Other Motor Neuron Disord 2003, 4, 191–206.
9. Rosen DR; Siddique T; Patterson D; Figlewicz DA; Sapp P; Hentati A; Donaldson D; Goto J; O’Regan JP; Deng H; Rahmani Z; Krizus A; Mckenna-Yasek D; Cayabyab A; Gaston SM; Berger R; Tanzi RE; Halperin JJ; Herzfeldt B; Van den Bergh R; Hung W; Bird T; Deng G; Mulder DW; smyth C; Laing NG; Soriano E; Pericak-Vance MA; Haines J; Rouleau GA; Gusella J; Horvitz HR; Brown RH Jr. Mutations in Cu/Zn superoxide dismutase gene are associated with familial amyotrophic lateral sclerosis. Nature 1993, 362, 59–62. [PubMed: 8446170]
10. Pasinelli P; Brown RH Molecular biology of amyotrophic lateral sclerosis: insight from genetics Nat. Rev. Neurosci 2006, 7, 710–723. [PubMed: 16924260]
11. Mulder DW; Kurland LT; Offord KP; Beard CM Familial adult motor neuron disease: amyotrophic lateral sclerosis. Neurology 1986, 36, 511–517. [PubMed: 3960325]
12. Pramatarova A; Figlewicz DA; Krizus A; Han FY; Ceballos-Picot I; Nicole A; Dib M; Meininger V; Brown RH; Rouleau GA Identification of new mutationsin the Cu/Zn superoxide dismutase gene of patients with familial amyotrophic lateral sclerosis. Am. J. Hum. Genet 1995, 56, 592–596. [PubMed: 7887412]
13. Ryu H; Ferrante RJ Translational therapeutic strategies in amyotrophic lateral sclerosis. Mini-Reviews Med. Chem 2007, 7, 141–150.
14. Andersen PM; Sims KB; Xin WW; Kiely R; O’Neill G; Ravits J; Pioro E; Harati Y; Brower RD; Levine JS; Heinicke HU; Seltzer W; Boss M; Brown RH Jr. Sixteen novel mutations in the Cu/Zn superoxide dismutase gene in amyotrophic lateral sclerosis: a decade of discoveries, defects and diputes. Amyotroph. Lat. Scler. Other Motor Neuron Disord 2003, 4, 62–73.
15. Brown RH Jr.; Robberecht W Amyotrophic lateral sclerosis: pathogenesis. Semin. Neurol 2001, 21, 131–139. [PubMed: 11442322]

16. Newbery HJ; Abbott CM Of mice, men and motor neurons. Trends Mol. Med 2002, 8, 88–92. [PubMed: 11815275]

17. Bruijn LI; Houseweart MK; Kato S; Anderson KL; Anderson SD; Ohama E; Reaume AG; Scott RW; Cleveland DW Aggregation and Motor Neuron Toxicity of an ALS-linked SOD1 Mutant Independent from Wild-type SOD1. Science 1998, 281, 1851–1854. [PubMed: 9743498]

18. Matsumoto G; Stojanovic A; Holmber CI; Kim S; Morimoto RI Structural Properties and Neuronal Toxicity of Amyotrophic Lateral Sclerosis-associated Cu/Zn Superoxide Dismutase 1 Aggregates. J. Cell Biol 2005, 171, 75–85. [PubMed: 16216923]

19. Matsumoto G; Kim S; Morimoto RI Huntingtin and mutant SOD1 form aggregate structures with distinct molecular properties in human cells. J. Biol. Chem 2006, 281, 4477–4485. [PubMed: 16371362]

20. Benmohamed R; Arvanites AC; Silverman RB; Morimoto RI; Ferrante RJ; Kirsch DR Identification of compounds protective against G93A SOD1 toxicity for the treatment of amyotrophic lateral sclerosis. Amyotroph. Lat. Scler. Other Motor Neuron Disord 2011, 12, 87–96.

21. Chen T; Benmohamed R; Arvanites AC; Ranaivo HR; Morimoto RI; Ferrante RJ; Watterson DM; Kirsch DR; Silverman RB Arylsulfanyl pyrazolones block mutant SOD1-G93A aggregation. Potential application for the treatment of amyotrophic lateral sclerosis. Bioorg. Med. Chem 2011, 19, 613–622. [PubMed: 21095130]

22. Basak A; Barlan AU; Yamamoto H Catalytic enantioselective oxidation of sulfides and disulfides by a chiral complex of bis-hydroxamic acid and molybdenum. Tetrahedron: Asymmetry 2006, 17, 508–511.

23. Zhang W; Yamamoto H Vanadium-catalyzed asymmetric epoxidation of homoallylic alcohols. J. Am. Chem. Soc 2007, 129, 286–287. [PubMed: 17212403]

24. Sonda S; Kawahara T; Murozono T; Sato N; Asona K; Haga K Design and synthesis of orally active benzamide derivatives as potent serotonin 4 receptor agonist. Bioorg. Med. Chem 2003, 11, 4225–4234. [PubMed: 12951153]

25. Banfi L; Casicio G; Ghiron C; Guanti G; Manghisi E; Narisano E; Riva R Microbiological enatioselecrive synthesis of (S) and (R) 4-(p-anisyloxy)-3-hydroxybutyrates as new chiral building blocks for the synthesis of β-lactam antibiotics. Tetrahedron 1994, 50, 11983–11994.

26. Hirner S; Panknin O; Edefuhr M; Somfai P Synthesis of aryl glycines by the α arylation of weinreb amides. Angew. Chem. Int. Ed 2008, 47, 1907–1909.

27. Gu R; Hameurlaine A; Dehaen W Facile one-pot synthesis of 6-monosubstituted and 6,12-disubstituted 5,11-dihydroindolo[3,2-*b*]carbazoles and preparation of various functionalized derivatives. J. Org. Chem 2007, 72, 7207–7213. [PubMed: 17696477]

28. Doherty EM; Fotsch M; Bo Y; Chakrabarti PP; Chen N; Gavva N; Han N; Kelly MG; Kincaid J; Klionsky L; Liu Q; Ognyanov VI; Tamir R; Wang X; Zhu J; Norman MH; Treanor JJS Discovery of potent, orally available vanilloid receptor-1 antagonists. structure−Activity relationship of *N*-aryl cinnamides. J. Med. Chem 2005, 48, 71–90. [PubMed: 15634002]

29. Hillier MC; Davidson JP; Martin SF Cyclopropane-derived peptidomimetics. design, synthesis, and evaluation of novel ras farnesyltransferase inhibitors. J. Org. Chem 2001, 66, 1657–1671. [PubMed: 11262110]

30. Nakajima T; Wang R; Elovaara E, Gonzalez F.J.; Gelboin H.V.; Raunio H.; Pelkonen O.; Vainio H.; Aoyama T. Toluene metabolism by cDNA-Expressed human hepatic cytochrome P450. Biochem. Pharmacol 1997, 53, 271–277. [PubMed: 9065730]

31. McNaney CA; Drexler DM; Hnatyshy SY; Zvyaga TA; Knipe JO; Belcastro JV; Sanders M An automated liquid chromatography-mass spectrometry process to determine metabolic stability half-life and intrinsic clearance of drug candidates by substrate depletion. Assay Drug Dev. Techol 2008, 6, 121–129.

32. (a)Mitchell SC; Waring RH The early history of xenobiotic sulphoxidation. Drug Metab. Rev. 1985, 16, 255–284. [PubMed: 3914937] (b)Fruetel J; Chang Y; Collins J; Loew G; Ortiz de Montellano PR Thioanisole sulfoxidation by cytochrome P450cam (CYP101): experimental and calculated absolute stereochemistries. J. Am. Chem. Soc 1994, 116, 11643–11648.

33. Kerns EH; Di L Drug-like Properties: Concepts, Structure, Design, and Methods; Elsevier, Inc.; Amsterdam, 2008; pp. 291.
34. Zhang W; Benmohamed R; Arvanites AC; Morimoto RI; Ferrante RJ; Kirsch DR; Silverman RB Cyclohexane 1,3-diones and their inhibition of mutant SOD1-dependent protein aggregation and toxicity in PC12 cells. Bioorg. Med. Chem, in press.
35. Kerns EH; Di L Drug-like Properties: Concepts, Structure, Design, and Methods; Elsevier, Inc.: Amsterdam, 2008; pp. 378.
36. Kerns EH; Di L Drug-like Properties: Concepts, Structure Design and Methods; Elsevier, Inc.: Amsterdam, 2008; pp. 288–291.
37. Press B; Di Grandi D Permeability for intestinal absorption: Caco - 2 assay and related issues. Curr. Drug Metab 2008, 9(9), 893–900. [PubMed: 18991586]
38. Ilieva H; Polymenidou M; Cleveland DW Non—Cell Autonomous Toxicity in Neurodegenerative Disorders: ALS and Beyond. J. Cell. Biol 2009, 187, 761–772. [PubMed: 19951898]
39. Talber AM; Transter GE; Holmes E; Francis PL Determination of drug-plasma protein binding kinetics and equilibria by chromatographic profiling: exemplification of the method using L-tryptophan and albumin. Anal. Chem 2002, 74, 446–452. [PubMed: 11811421]
40. Weisiger RA Dissociation from albumin: a potentially rate-limiting step in the clearance of substances by the liver. Proc. Natl. Acad. Sci. USA. 1985, 82, 1563–1567. [PubMed: 3856281]
41. (a)Kerns EH; Di L Drug-like Properties: Concepts, Structure, Design, and Methods; Elsevier, Inc.: Amsterdam, 2008; p. 234.(b)Mei H; Korfmacher W; Morrison R Rapid in vivo oral screening in rats: reliability, acceptance criteria, and filtering efficiency. AAPS J 2006, 8, E493–E500. [PubMed: 17025267]
42. (a)Bambal RB; Clarke SE Cytochrome P450: structure, function and application in drug discovery and development. Eval. Drug Cand. Preclin. Develop 2010, 55–107.(b)Wang B; Zhou S-F Synthetic and natural compounds that interact with human cytochrome P450 1A2 and implications in drug development. Curr. Med. Chem 2009, 16(31), 4066–4218. [PubMed: 19754423]
43. Nagai M; Aoki M; Miyoshi I; Kato M; Pasinelli P; Kasai N; Brown RH Jr.; Itoyama Y Rats expressing human cytosolic copper-zinc superoxide dismutase transgenes with amyotrophic lateral sclerosis: associated mutations develop motor neuron disease. J. Neurosci 2001, 21, 9246–9254. [PubMed: 11717358]
44. Aoki M; Kato S; Nagai M; Itoyama Y Development of a rat model of amyotrophic lateral sclerosis expressing a human SOD1 transgene. Neuropathology 2005, 25, 365–370. [PubMed: 16382787]
45. Gurney ME; Pu H; Chiu AY; Dal Canto MC; Polchow CY; Alexander DD; Caliendo J; Hentati A; Kown YW; Deng HX; Chen W; Zhai P; Sufit RL; Siddique T Motor neuron degeneration in mice that express a human Cu, Zn superoxide dismutase mutation. Science 1994, 264, 1772–1775. [PubMed: 8209258]
46. Del Signore SJ; Amante DJ; Km J; Stack EC; Goodrich S; Cormier K; Smith K; Cudkowicz ME; Ferrante RJ Combined riluzole and sodium phenylbutylrate therapy in transgenic amyotrophic lateral sclerosis mice. Amyotroph. Lat. Scler. Other Motor Neuron Disord 2009, 10, 85–94.
47. Gurney ME; Cutting FB; Zhai P; Doble A; Taylor CP; Andrus PK; Hall ED Benefit of vitamin E, riluzole, and gababapentin in a transgenic model of familial amyotrophic lateral sclerosis. Ann. Neurol 1996, 39, 147–157. [PubMed: 8967745]

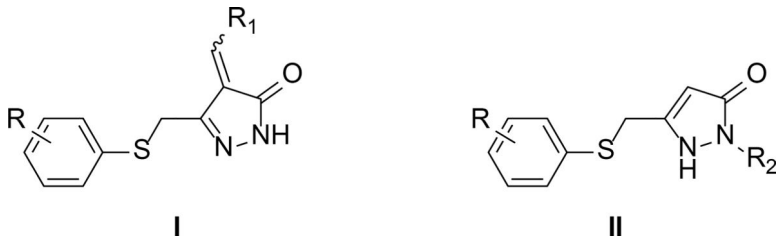

Figure 1.

ASP HTS hits. R_1, alkyl or substituted aromatic groups; R_2, proton or substituted aromatic groups; R, various alkyl and/or halogen groups.

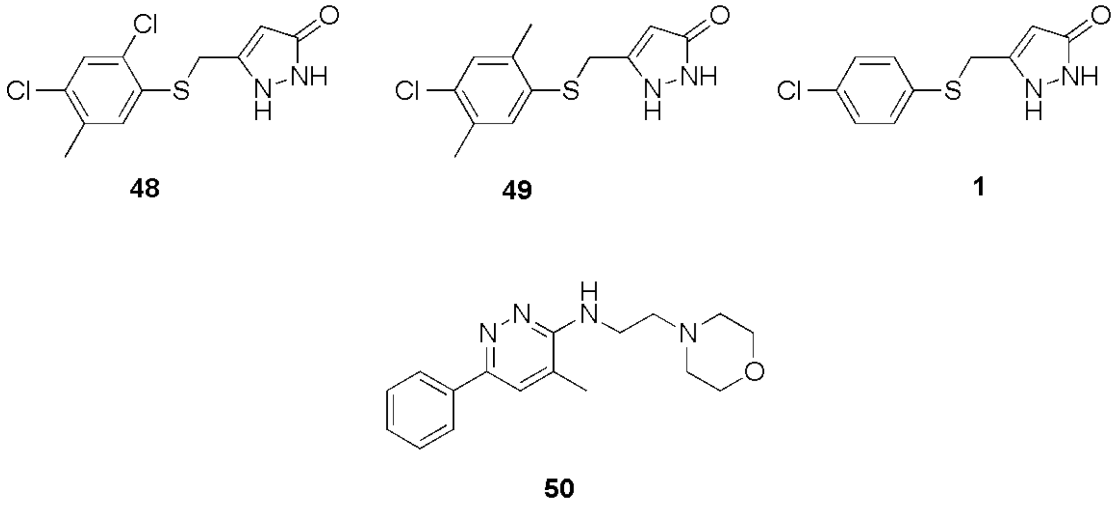

Figure 2.
Compounds tested in metabolic studies.

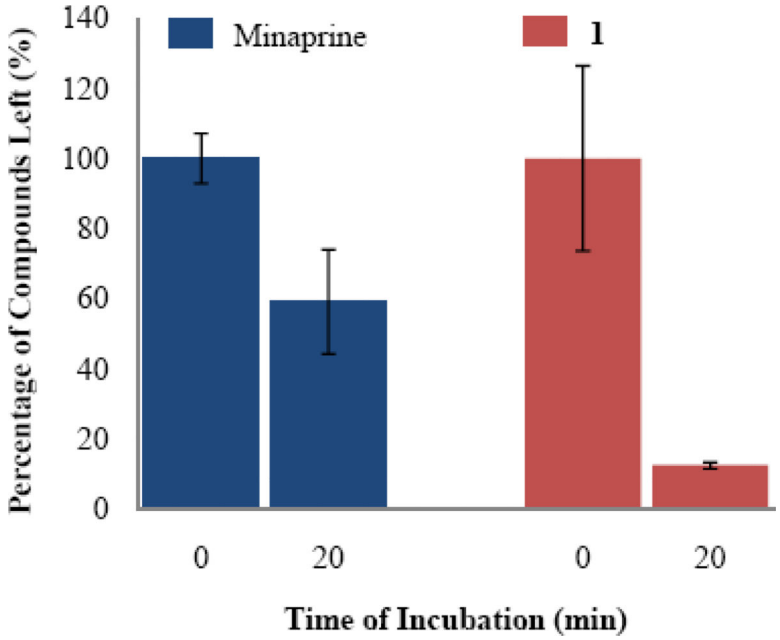

Figure 3.

Microsomal stability of minaprine (**50**) and **1**. Rat liver microsomes were incubated at 37 °C for 20 minutes in the presence of 15 μM compound.

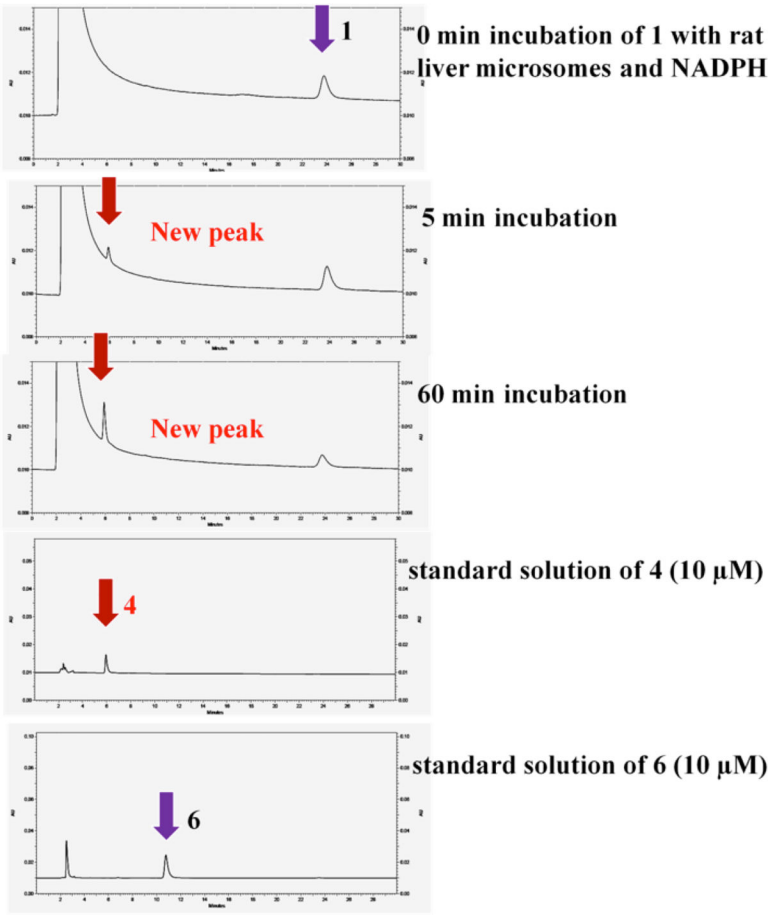

Figure 4.

HPLC traces of the incubation of **1** (15 μM) with rat liver microsomes at 37 °C

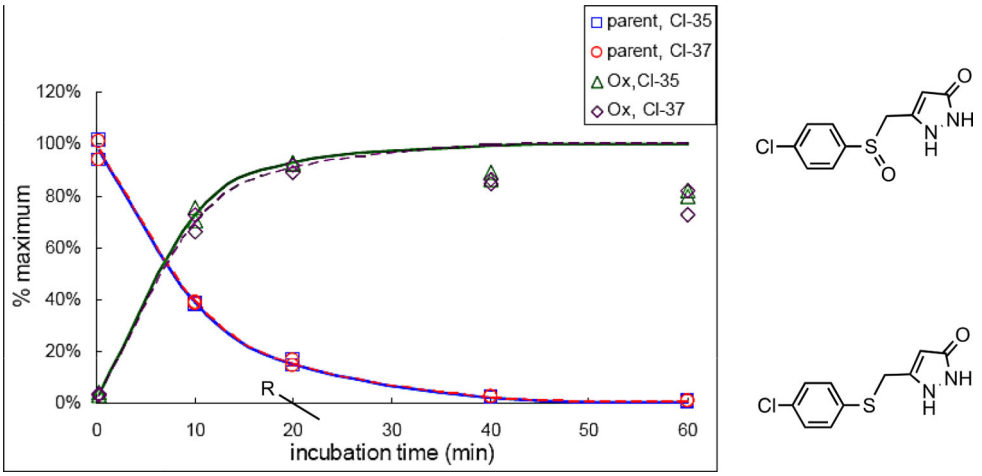

Figure 5.

Rate of formation of sulfoxide **4** and rate of metabolism of **1**

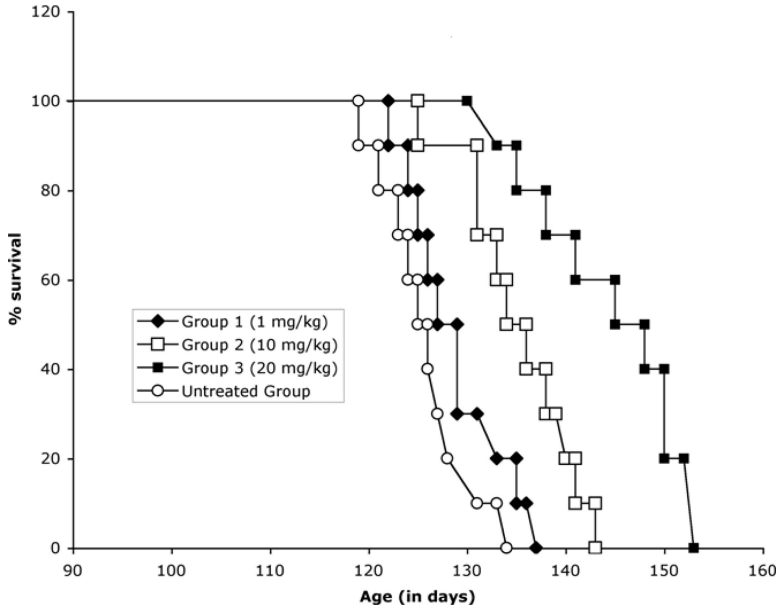

Figure 6.

Kaplan-Meier plot of **13**-treated SOD1 G93A ALS mice. Untreated Group: 125.7+/−4.9 d; Group 1 (1 mg/kg): 129.2+/−5.3 d; Group 2 (10 mg/kg): 135+/−5.5 d; Group 3 (20 mg/kg): 142.5+/−8.2 d; $p < 0.05$.

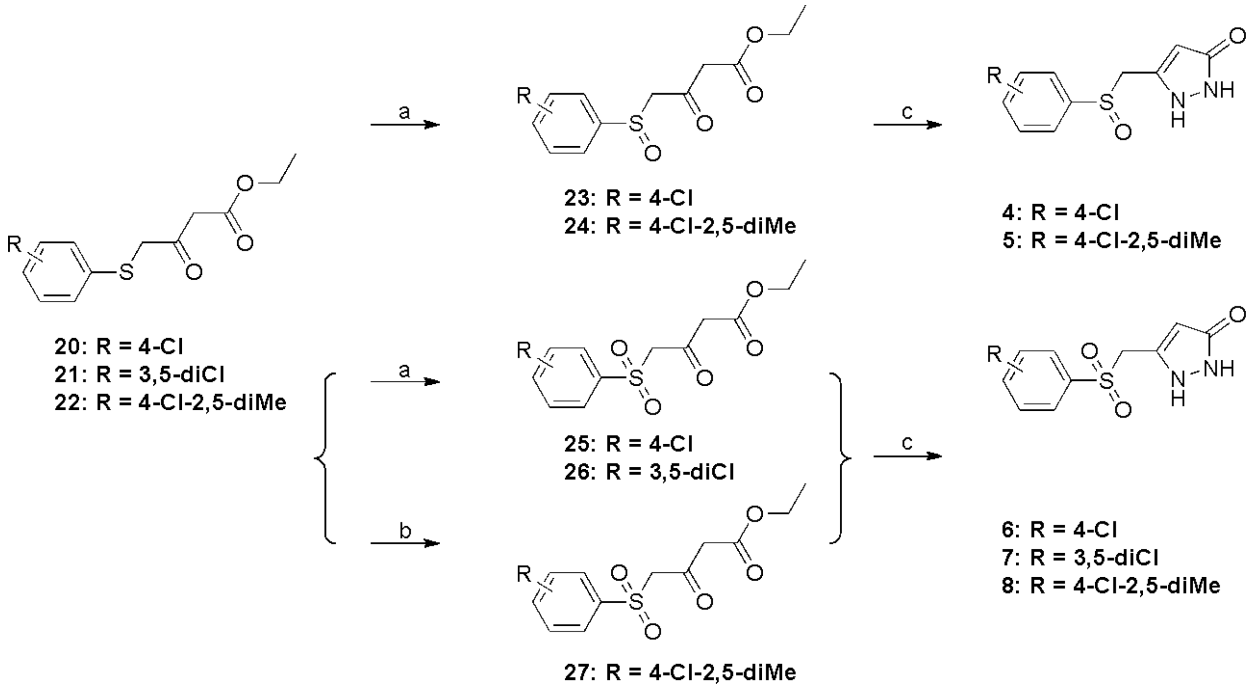

Scheme 1[a]

[a]Reagents and conditions: (a) TBHP, $VO(acac)_2$, DCM, room temperature, overnight; (b) H_2O_2, AcOH, EtOAc, room temperature; (c) NH_2NH_2, EtOH, room temperature, overnight.

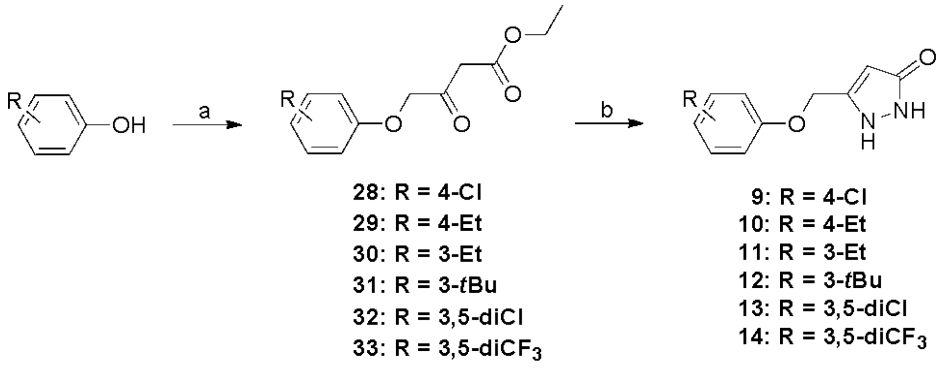

Scheme 2[a]

[a]Reagents and conditions: (a) ethyl 4-chloroacetoacetate, NaH, THF, DMF, −20 °C to 70 °C; (b) NH_2NH_2, EtOH, room temperature, overnight.

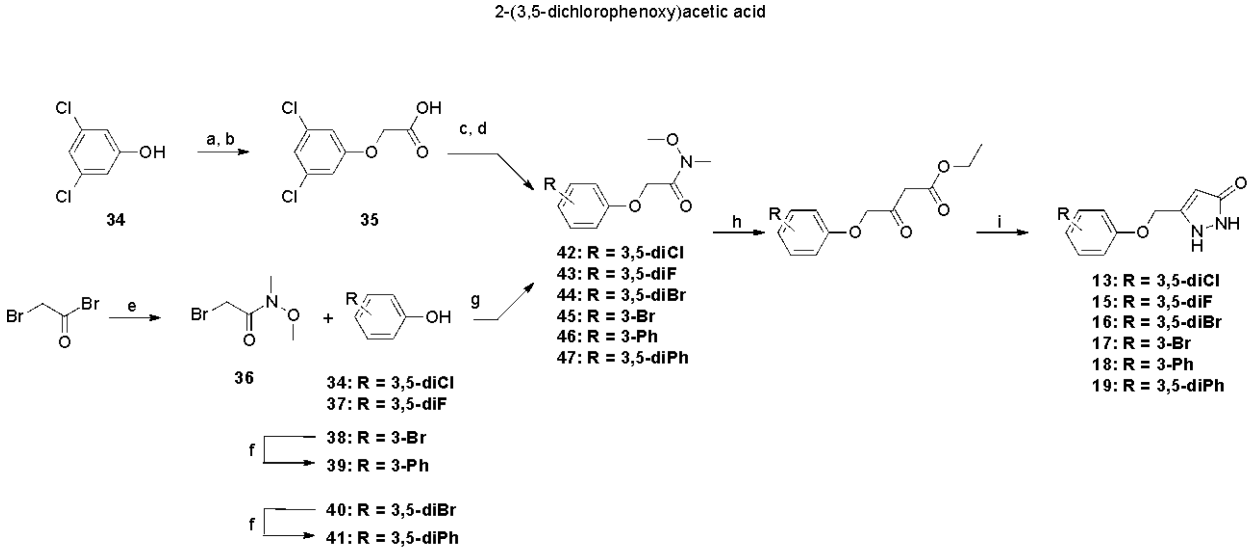

Scheme 3[a]

[a]Reagents and conditions: (a) ethyl 2-bromoacetate, NaOEt, EtOH, reflux, overnight; (b) NaOH, H_2O, 80 °C, overnight; (c) oxalyl chloride, DCM, DMF, room temperature, 4 h; (d) *N,O*-dimethylhydroxylamine hydrochloride, DIEA, DCM, room temperature, 1 h; (e) *N,O*-dimethylhydroxylamine hydrochloride, K_2CO_3, Et_2O, H_2O, room temperature, 30 min; (f) phenylboronic acid, $PdCl_2(PPh_3)_2$, K_2CO_3, dioxane, H_2O, 100 °C, 16 h; (g) NaOEt, EtOH, 70 °C, overnight; (h) EtOAc, LiHMDS, THF, −78 °C, overnight; (i) NH_2NH_2, EtOH, room temperature, overnight.

Table 1.

SAR of ASP analogs with -S-, -SO-, -SO_2-, and -O- linkers[a]

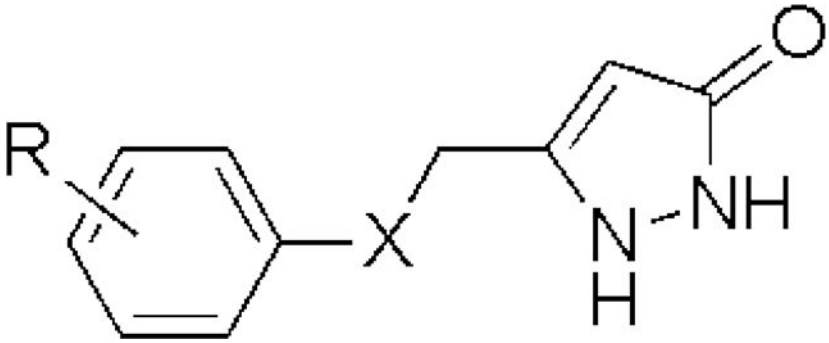

X	Compound	R	EC_{50} (μM)
S	**1**	4-Cl	1.93
	2	2.6-diCl	0.71
	3	3,5-diCl	0.17
SO	**4**	4-Cl	> 32
	5	4-Cl-2,5-diMe	2.88
SO_2	**6**	4-Cl	4.7
	7	3,5-diCl	1.41
	8	4-Cl-2,5-diMe	1.47
O	**9**	4-Cl	0.79
	10	4-Et	1.96
	11	3-Et	0.72
	12	3-*t*-Bu	0.87
	13	3,5-diCl	0.067
	14	3,5-diCF_3	0.58
	15	3,5-diF	1.07
	16	3,5-diBr	0.51
	17	3-Br	1.02
	18	3-Ph	2.84
	19	3,5-diPh	3.70

[a]Average Z' factor value = 0.5

Table 2.

In Vitro Microsomal Stability of **7**, **9**, and **13**.

Compd	Human			Mouse		
	CL'_{int} [a] (mL/min/kg)	$T_{1/2}$ [b] (min)	CL'_{int} NADPH-free (mL/min/kg)	CL'_{int} (mL/min/kg)	$T_{1/2}$ (min)	CL'_{int} NADPH-free (mL/min/kg)
7	4.5	> 60	1.3	15.3	> 60	0
9	15.3	139	0	24.5	143	6.1
13	25	93	13	64	36	21

[a] Microsomal intrinsic clearance.

[b] Half-life.

[c] Experimental procedures and data analysis are described in reference 29. Data were obtained from Apredica and Biogen Idec.

Table 3.

In Vitro Aqueous Solubility of Compounds **7**, **9**, and **13**[a]

Compound	Maximum Solubility (μM)	
	45 min	16 h
7	≥500	≥500
9	250	250
13	250	250

[a]Data were obtained at Apredica Inc. Experimental procedures and data analysis are described in reference 21.

Table 4.

In Vitro Caco-2 Permeability of **7**, **9**, and **13**[a]

Compd	P_{app}[b] (A→B) (10^{-6} cm/s)	P_{app} (B→A) (10^{-6} cm/s)	Ratio (B→A / A→B)
7	27.0	4.4	0.2
9	43.0	28.0	0.6
13	36.7	14.1	0.4

[a] Data were obtained from Apredica Inc. Experimental procedures and data analysis are described in reference 21.

[b] Apparent permeability.

Table 5.

In Vivo Plasma Concentration of Compound **13**[a]

Time (h)	Plasma Concentration (μg/mL; [μM]}
0	0
3	88.8 [342]
6	90 [347]
12	64.4 [248]
24	1.7 [6.5]

[a]Brain and plasma samples were analyzed at Apredica, Inc.

Table 6.

Rat Plasma PK Profile of Compound **13**[a]

	AUC Last (ng × h/mL)	AUC/Dose (ng × h/mL/dose)	$T_{1/2}$ (h)	CL (mL/min/kg)	Vss (L/kg)	C_{max} (ng/mL)	T_{max} (h)	F (%)
i.v.	179	184	2.1	92	5.7	-	-	-
p.o.	42	50	3.6	-	-	39	0.25	27

[a]Single bolus administration of 1 mg/kg i.v. and p.o. to SD rats; data were obtained from Biogen Idec.